Response to Anonymous Referee #2

The manuscript by Heinemann et al., describes the addition of a ballasting parameterisation within the MPI-OM/HAMOCC model and is used to quantify the contribution of ballasting to glacial-interglacial changes in CO_2 associated with changing dust fluxes. The authors find that ballasting by dust particles has a smaller drawdown of atmospheric CO_2 compared with the effect of iron fertilisation when forced with glacial dust fluxes. I think this is a really interesting question to explore as there has been comparatively less focus on processes affecting organic carbon fluxes in the ocean interior than on the effects of iron fertilisation. However, I think it's difficult to reach a satisfying answer because the iron fertilisation effect in these experiments does not occur in the Southern Ocean as generally understood by the iron hypothesis. The authors are open about this in the manuscript but ultimately I think this limits the findings. I have detailed a number of comments on this as well as the ballasting parameterisation and sediment model below. If the authors are able to address this key issue then I think the manuscript would suitable for publication.

General Comments:

The modelled iron fertilisation effect in the model does not occur in the Southern Ocean as understood by the iron hypothesis. This has a number of issues for interpreting the results. Firstly, CO_2 drawdown associated with export production varies by location (DeVries et al., 2012) and therefore the CO_2 sensitivity for the iron fertilisation experiments may not be comparable. The sensitivity falls below the cited range in the introduction (8 ppm vs. 15-40 ppm).

We agree with the reviewer and think that the presented CO_2 sensitivity for the iron fertilization is not comparable to the range cited in the introduction, because non-diazotrophic phytoplankton is not iron limited anywhere in our control simulations. We still think that presenting the iron sensitivity results is interesting enough, illustrating the effect of iron fertilization on cyanobacteria.

Secondly, changes in ballasting and sinking rates will lead to changes in nutrient distributions which could potentially enhance or reduce any export production changes associated with iron fertilisation. For example, an increase in export production with iron fertilisation may be reduced if ballasting increases sinking speeds locally relocating nutrients within the water column. For these reasons, I think the comparison of CO_2 changes is hard to interpret fully.

We will point out in the revised manuscript that, when comparing the effects of iron fertilization and ballasting, potential interactions between the two effects such as in the given example have to be kept in mind. The given example effect could potentially be one contributor to the fact that the sum of the ballasting effect and the iron fertilization effect on

CO_2 is slightly larger than their combined effect on CO_2 (Fig. 3).

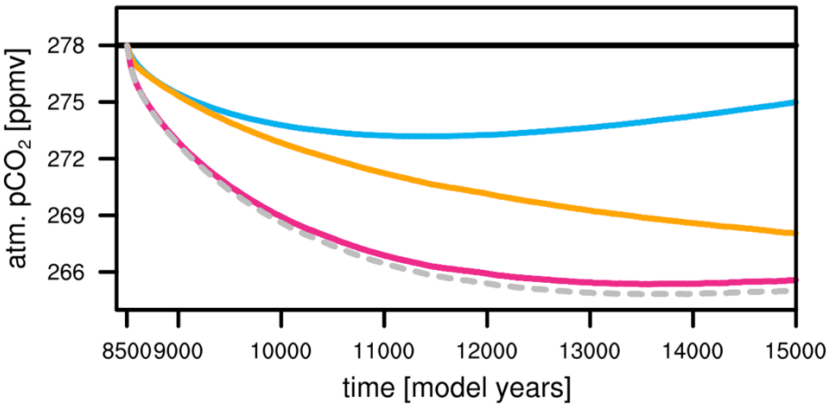

Figure 3: Sum of ballasting effect and iron fertilization effect on atmospheric pCO_2 (grey dashed line) compared to the fertilization effect alone (orange; LGM_IRON), the ballasting effect alone (blue; LGM_BALL), and the combined effect (pink; LGM_BOTH).

The description of the ballasting scheme, its appropriateness and impacts needs better description overall. The scheme from Gehlen et al., (2006) assigns a single sinking rate to all particle types according to the average excess density particles. While this scheme has been used previously, I think a few things need discussion: this scheme assumes a key role for particle aggregation (this is really a ballasting and aggregation parameterisation) and that this scheme differs considerably from other ballasting schemes used previously, (Howard et al., 2006; Hoffman and Schellnhuber 2009).

In the revised manuscript, we will discuss the differences of our ballast parameterization as compared to the schemes / type of schemes used by Klaas and Archer (2002), Howard et al. and Hofmann and Schellnhuber. As detailed in the specific comments below, we will also discuss the lack of an explicit aggregation scheme.

Given the significant impact on opal sinking rates, I think this needs some thought. Additional figures, such as Taylor diagrams showing statistical fits for the new and old scheme versus observations would help assure me this scheme is working well.

We will add a Taylor diagram to the revised manuscript, showing statistical fits of nutrient concentrations, including silicate, for both schemes versus World Ocean Atlas data (Fig. 4). For silicate, the diagram illustrates that the magnitude of spatial variability of the silicate distribution in the run with ballasting is closer to observations, while the correlation with observations hardly differs.

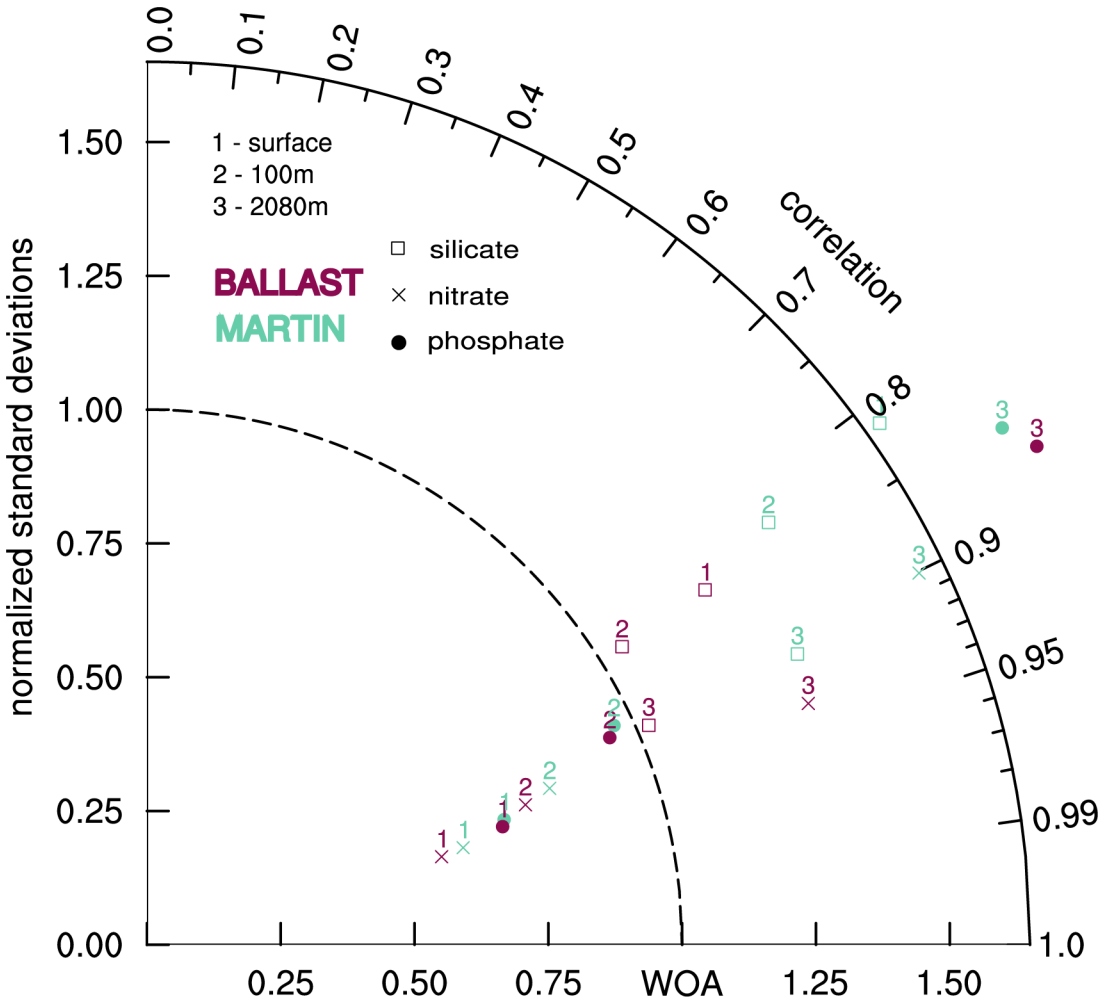

Figure 4: Taylor diagram comparing annual mean silicate (squares), nitrate (crosses), and phosphate concentrations (dots) at 3 different depths (numbers) of the preindustrial reference simulations with Martin-type sinking (MARTIN, aquamarine) and with particle ballasting (BALLAST, pink) to World Ocean Atlas data (WOA; Garcia et al. 2013).

Please also state all the units when describing the ballasting parameterisation.

We will add that the mass concentration c_dust is the mass of dust per unit volume of seawater (e.g., in g per cm3 seawater), and that the molar concentrations PSI_b are given in mol C and mol Si per unit volume of seawater respectively (e.g., for PSI_detritus and PSI_calcite in mol C per cm3 seawater).

The inclusion of sediments here is not well described or justified. The experiments don't seem to have reached a steady-state (e.g.,Figure 4a), is this because the sediments are still responding? Depending on the processes in the sediment model, there could be different responses to iron fertilisation and ballasting as ballasting will affect the ratios of particulate matter reaching the seafloor (e.g., Ridgwell 2003). Would it be possible to isolate and quantify the effect of sediments on the CO_2 drawdown?

Regarding the long-term trends seen in Fig. 4a, the strongest trend in atmospheric pCO_2 occurs in the iron fertilization experiment, and we attribute this long-term trend to a continuously reduced PIC/POC ratio of the export production relative to the reference

simulation, and hence a continuously reduced export of alkalinity, while the PIC/POC ratio in the LGM ballast simulation increases again over time due to reduced primary productivity in response to nitrate depletion (see Fig. 2 in our response to Referee #1).

However, it is still possible that changes in the sediment are contributing to the simulated long-term trend, and we will discuss this possibility in the revised manuscript. Quantifying this contribution is difficult, because the equilibration time with the sediment is very long, and equilibrium in the sediment has hardly been reached in the presented sensitivity simulations (see, e.g., the positive trend of calcite fluxes into the sediment, Fig. 5b), although we extended all sensitivity runs by another 2000 years. We do see that, despite the enhanced export production in the iron fertilization experiment (due to the enhanced cyanobacterial growth; Fig. 4c in the manuscript), the detritus flux into the sediment in that simulation is smaller than in the reference run without the extra iron (Fig. 5a), suggesting that detritus burial is not contributing to the long-term atmospheric CO_2 trend in the LGM iron simulation.

The standard version of MPIOM/HAMOCC does come with the activated sediment module, which was described briefly in Section 2.3 of Ilyina et al. (2013), or more extensively by Heinze et al. (1999). If it had been easily possible, we would have preferred to first turn off interactions of the ocean column with the sediment to avoid this problem. In future studies, an offline version of the sediment module that was recently developed at the MPI for Meteorology can be used to accelerate this equilibration process (for example to achieve equilibrium for the LGM, before a transient deglaciation simulation is started).

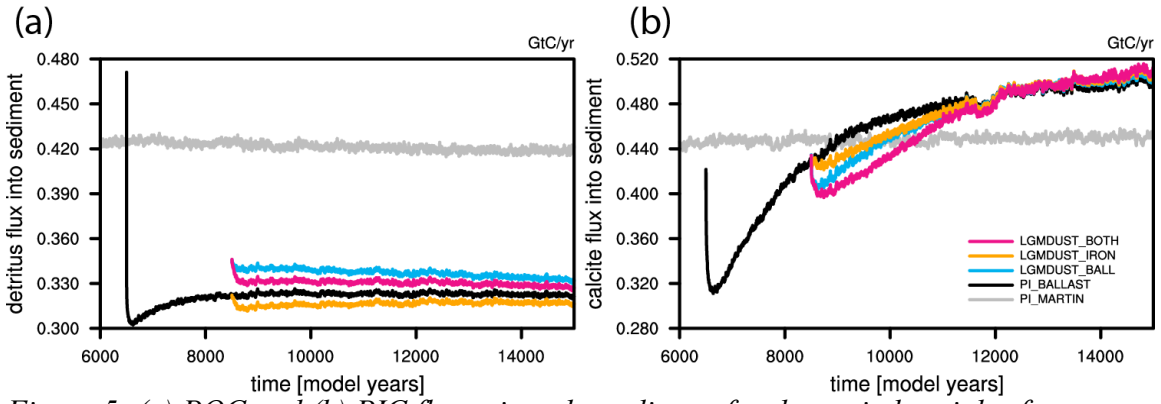

Figure 5: (a) POC and (b) PIC fluxes into the sediment for the preindustrial reference runs with Martin-type sinking (gray) and with particle ballasting (black), as well as for the LGM dust sensitivity experiments using the dust only for ballasting (blue; LGM_BALL), only for iron fertilization (orange; LGM_IRON), and for both (pink; LGM_BOTH).

Specific Comments:

Pg 2, lines 20 - 30: The citations for dust/lithogenic ballasting seem limited to only a few papers (Klaas and Archer 2002; Dunne et al., 2007) with a lack of more recent papers focussing on observed effects.

We will add more recent references in the revised manuscript (e.g., van der Jagd et al. 2018).

Pg 3, line 14: I am not sure the experiments here can be called equilibrium experiments as atmospheric CO_2 still seems to be changing in Figure 4a, and as also mentioned at the bottom of page 5.

Agreed. The word "equilibrium" will be omitted in the revised manuscript.

Pg 3, line 33: The description of the box model of atmospheric CO_2 referred to here is quite limited. The description later on might be better located here.
We will move parts of Section 4.2 / the general description of the box model here.

Pg 4, lines 3-5: This is quite a lot of description of the grid-setup, does it have implications or relevance for the interpretation of the results?
The model grid-setup needs to be at least mentioned, since several pre-defined MPIOM grid setups exist. Some model parameters are set according to the resolution – for example the primary production depends on the thicknesses of the top layers (because growth rates are computed using the insolation at the top of each box). We will shorten the description in the revised manuscript.

Figure 2: It might be helpful to also see the global flux profile, e.g., a Martin Curve equivalent, to get a handle on how the sinking speeds contribute to changes in particulate fluxes.
A Martin-curve-equivalent will be added in the revised manuscript, illustrating that the global fluxes are enhanced above 2000m depth by the higher mean sinking speed in the simulation with ballasting (Figure 6).

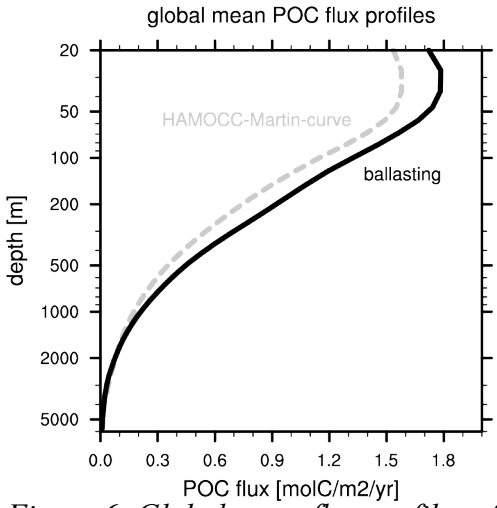

Figure 6: Global mean flux profiles of particulate organic carbon for the modern control simulation with Martin-type sinking (gray dashed) and the simulation with particle ballasting (black).

Pg 7, lines 9-10: a change in the sinking rate for opal from 30 m day^{-1} to 5 m day^{-1} is quite dramatic. I would like some discussion about this change, e.g., how does it compare to values in literature and other models? Is this scheme better because of the explicit use of density or are there other things missing? Adding some summary plots about different tracers (see general comments) would also help clarify the impact of this change.

We will discuss the advantages and potential disadvantages or improvements of the ballasting scheme in more detail in the revised manuscript. The explicit calculation of the excess density allows us to test the ballasting hypothesis. As already mentioned in the manuscript, one potential improvement would be the inclusion of aggregate porosity. The effect of particle size is also missing in our parameterization – although we do know that, according to Stokes' drag, sinking velocities tend to increase with particle size. We will also discuss in more detail that the ballasting parameterization basically assumes instant formation of aggregates with the computed density, neglecting the complex biological and physical

aggregation and disaggregation processes that occur in reality (e.g., Lam and Marchal 2015) or that are explicitly captured in more complex (and computationally more expensive) aggregation models (e.g., Kriest and Evans 2000).

We would like to emphasize that the reduction of the opal sinking speed from the prescribed value of 30m/day to about 5m/day (as opal sinking within the virtual aggregates) only occurs in the euphotic zone. The sinking speed increases with depth to about 20m/day at 1km depth, to 30m/day at 3km, and to as much as 120m/day below 5km depth (within the virtual aggregate; black curve in Fig. 2a in the manuscript).

Still, the sinking speeds are small compared to, e.g., those in the ocean biogeochemical model PISCES-v2 (Aumont et al., 2015), where the speed increases from about 50m/day at the surface to about 240m/day close to 5km depth. However, also the opal dissolution rates differ between the models, with a more complex formulation in PISCES depending on temperature and saturation states, resulting in rates up to 0.025 day^{-1}, which is 2.5 times faster than the standard remineralization in HAMOCC, and 15 times faster than the rate used in our simulations with ballasting.

The better fit to observations of the simulated silicate concentrations in our simulations with ballasting compared to the standard version of HAMOCC shows that the ballasting parameterization is an improvement over the standard opal sinking and remineralization parameterization (see Taylor-diagram above).

Pg 8, lines 15-20: no quantification of opal export here

Opal production (Fig. 1e in the manuscript) and opal export at 90m (not shown) are reduced by about 30 % in the simulation with modern dust and ballasting compared to the run without ballasting (production 76 versus 108 Tmol Si yr^{-1}, export 72 versus 103 Tmol Si yr^{-1}). We will add those numbers to the revised manuscript.

Pg 8, lines 26-29: As I understand, the sediment trap data presented in Honjo et al., (2008) is normalised to 2000 m using the Martin curve on the basis that gravitational settling is the dominant process at this depth. The data here is reported at 1000 m. Did you apply the same normalisation and if so can the same assumptions apply at this depth?

Indeed, we accidentally compared the data to the simulated 960m export instead of to the simulated export close to 2000m depth. We corrected our mistake (Figure 7), now comparing the transfer efficiency from Honjo et al. (export at 2000m depth divided by export at 100m depth) to the simulated transfer efficiency computed from the fluxes at 2080m and 100m depth. The simulated transfer efficiencies match the data from Honjo et al. much better now; the mistake explains why we previously overestimated the transfer efficiency.

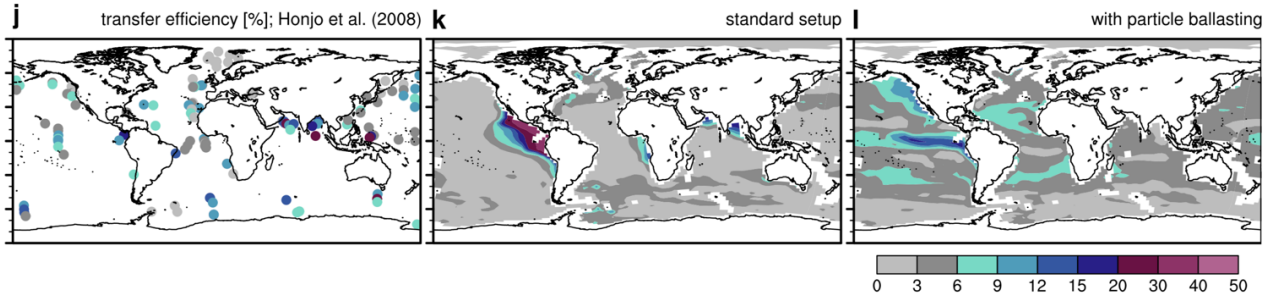

Figure 7: New Fig. 3 j-l. Transfer efficiency computed from Honjo et al. (2008, panel j), compared to the simulated transfer efficiencies in the control run with Martin-type sinking (k)

and the run with ballasting and modern dust deposition (l) computed as the fraction of detritus export at 2080m compared to 100m depth.

Figure 3: What causes the transfer efficiency pattern in the standard model (panel k)? From the previous description, it seems like this should be globally uniform.

The pattern arises because detritus remineralization rates depend on oxygen availability. Denitrification and sulfate reduction remineralization rates combined are lower than aerobic remineralization rates (see Eq. 6 of Ilyina et al., 2013), leading to higher transfer efficiencies in oxygen minimum zones (Figure 8 and Figure 7 (new Fig. 3k in manuscript)). In the simulations with particle ballasting, this effect of lower remineralization rates in oxygen minimum zones is partly compensated by reduced ballasting by calcite due to the corrosive waters, resulting in lower settling speeds and transfer efficiencies (Figure 7 (new Fig. 3l in manuscript)).

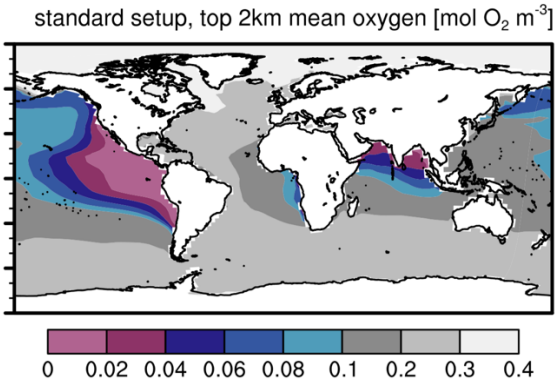

Figure 8: Mean oxygen concentration in the upper 2km of the water column in the modern control simulation without ballasting.

Pg 10, line 6: I think the comparison between the ballast scheme here and Weber et al., (2016) is unwarranted as this is not the focus of the manuscript. The Weber analysis derives from an inversion of nutrient distributions and so represents the net effect of any number of potential processes. Any differences might therefore reflect the importance of other processes other than ballasting in some regions.

We will focus on the comparison with direct flux data in the revised manuscript.

Pg 11, line 7: I am unfamiliar with this approach to modelling atmospheric CO_2, where does 2.1 Gt C / 1 ppm relationship derive from?

The relationship is an estimate based on the mass of the atmosphere, the molar masses of CO_2, C and air, and the assumption that the air and CO_2 in the atmosphere are ideal gases.

One ppmv of atmospheric CO_2 is equivalent to a volume of CO_2 = (volume of the atmosphere * 10^{-6}). Since the volume of a gas is given by its mass m times its molar volume divided by its molar mass M, and assuming that the molar volumes of CO_2 and air are the same (assuming that they are ideal gases), the mass m of CO_2 equivalent to 1ppmv is given by $m_{CO2\ 1ppm} = 10^{-6} * M_{CO2} * m_{atm} / M_{air}$, where M_{air} is the molar mass of dry air (28.96g/mol for 78.084% nitrogen, 20.946% oxygen, 0.934% argon and 0.03% CO_2), m_{atm} is the mass of the atmosphere (5.15×10^{18}kg, e.g., Trenberth and Smith, 2005), and M_{CO2} is the molar mass of

CO_2 (44g/mol), which yields $m_{CO2\_1ppm} \approx 7.82Gt$. 7.82Gt of CO_2 are equivalent to $7.82Gt * M_{CO2}/M_C \approx 7.82*44/12Gt \approx 2.13Gt$ of carbon.

Figure 4: The CO_2 drawdown for the iron fertilisation (8 ppm) is lower than the published range mentioned in the Introduction (15 - 40 ppm). This needs some discussion, see also general comments.

We will further clarify in the revised manuscript that the simulated iron fertilization effect is solely due to the fertilization of cyanobacteria growth, and not comparable to the previous estimates from the literature.

Pg 14, lines 1-3: Does the weakening of the calcite export reflect a shift towards silicifying organisms? If so, does this also have an effect on ballasting sinking rates? i.e., is there a dual effect of ballasting from dust and from opal? I think these effects are quite interesting!

We do see a shift towards silicifying organisms in the simulation with LGM dust for iron fertilization (LGM_IRON), as reflected by reduced calcite export (see Fig. 2b in response to the first reviewer) while opal export is enhanced (Fig. 9a, below). However, the global mean sinking speed in LGM_IRON hardly differs from that in the reference run with modern dust (PI_BALLAST; Fig. 9b), suggesting that the ballasting effect of the additional opal is balanced by the effect of the reduced calcite concentration.

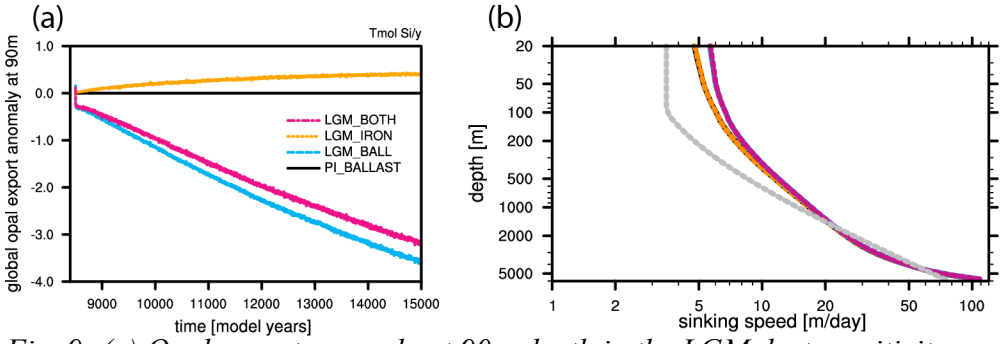

Fig. 9: (a) Opal export anomaly at 90m depth in the LGM dust sensitivity experiments using the dust only for ballasting (blue; LGM_BALL), only for iron fertilization (orange; LGM_IRON), and for both (pink; LGM_BOTH) relative to the pre-industrial reference with ballasting and modern dust (black, PI_BALLAST), and (b) global mean sinking speed profiles for the preindustrial reference run with particle ballasting (PI_BALLAST, black), and for the LGM sensitivity runs (colors as in panel a). For comparison, the gray dashed line in (b) is the applied Martin-type sinking speed in the PI reference run without ballasting.

References

DeVries et al., (2012) The sequestration efficiency of the biological pump. Geophysical Research Letters. 39 (13)

Hofmann and Schellnhuber (2009) Oceanic acidification affects marine carbon pump and triggers extended marine oxygen holes. PNAS. 106 (9)

Howard et al., (2006) Sensitivity of ocean carbon tracer distributions to particulate organic flux parameterizations. Global Biogeochemical Cycles. 20 (3)

Ridgwell (2003) An end to the "rain ratio" reign?. Geochemistry Geophysics Geosystems. 4 (6)

van der Jagt et al. (2018). The ballasting effect of Saharan dust deposition on aggregate dynamics and carbon export: Aggregation, settling, and scavenging potential of marine snow. Limnology and Oceanography, 63(3), 1386–1394. http://doi.org/10.1002/lno.10779
Trenberth, K. E., & Smith, L. (2005). The Mass of the Atmosphere: A Constraint on Global Analyses. *Journal of Climate*, *18*(6), 864–875. http://doi.org/10.1175/JCLI-3299.1

Heinze, C., Maier-Reimer, E., Winguth, A. M. E., & Archer, D. (1999). A global oceanic sediment model for long-term climate studies. Global Biogeochemical Cycles, 13(1), 221–250. http://doi.org/10.1029/98GB02812

Lam, P. J., & Marchal, O. (2015). Insights into Particle Cycling from Thorium and Particle Data. Annual Review of Marine Science, 7(1), 159–184. http://doi.org/10.1146/annurev-marine-010814-015623

Kriest, I., & Evans, G. T. (2000). A vertically resolved model for phytoplankton aggregation. Journal of Earth System Science, 109(4), 453–469. http://doi.org/10.1007/BF02708333